VU VRIJE UNIVERSITEIT AMSTERDAM

VU Research Portal

Sensory pathways of muscle phenotypic plasticity: Calcium signalling through CaMKII

Eilers, W.

2013

document version
Publisher's PDF, also known as Version of record

Link to publication in VU Research Portal

citation for published version (APA)
Eilers, W. (2013). *Sensory pathways of muscle phenotypic plasticity: Calcium signalling through CaMKII*.

General rights
Copyright and moral rights for the publications made accessible in the public portal are retained by the authors and/or other copyright owners and it is a condition of accessing publications that users recognise and abide by the legal requirements associated with these rights.

- Users may download and print one copy of any publication from the public portal for the purpose of private study or research.
- You may not further distribute the material or use it for any profit-making activity or commercial gain
- You may freely distribute the URL identifying the publication in the public portal ?

Take down policy
If you believe that this document breaches copyright please contact us providing details, and we will remove access to the work immediately and investigate your claim.

E-mail address:
vuresearchportal.ub@vu.nl

Download date: 06. Mar. 2021

Computational modelling of CaMKII activity and its effects on calcium dynamics in sarcomeres

Wouter Eilers, Willemijn Groenendaal, Richard T. Jaspers, Arnold de Haan, Natal A. van Riel & Martin Flueck

Abstract

Calcium/calmodulin-dependent protein kinase II (CaMKII) has been demonstrated to modulate calcium release from the sarcoplasmic reticulum and phosphorylate the sarco/endoplasmic reticulum Ca^{2+}-ATPase *in vitro*. CaMKII overexpression in skeletal muscle *in vivo* increased twitch contraction and relaxation speed (chapter 3). However, it is unclear if CaMKII-dependent modification of RyR and SERCA activity is sufficient to explain the increase twitch speed. In addition, it is unclear if CaMKII activation is similar throughout the subsarcomeric space or if activation is higher near the calcium release sites. To address these questions, we used a mathematical model of spatiotemporal sarcomeric [Ca^{2+}] dynamics coupled to a biochemical model of CaMKII activation. Modelling results were compared to experimental results. The model predicted substantial spatial gradients in CaMKII activity in sarcomeres of fast- and slow-twitch muscle fibres during single and repeated RyR openings. Increasing the CaMKII concentration in the model did not produce faster twitch speeds, which could be explained by minimal CaMKII activation during twitch contraction. Experimental overexpression of CaMKII increased SERCA2 expression in rat *m. soleus* muscle fibres and this could at least partially explain the observed decrease in twitch relaxation time (chapter 3). We conclude that not an increased CaMKII-dependent SERCA activity, but increased SERCA protein level underlies the increase in twitch relaxation speed after CaMKII overexpression.

Introduction

In skeletal muscle, calcium/calmodulin-dependent protein kinase II (CaMKII) is presumed to regulate calcium release from, and re-uptake into, the sarcoplasmic reticulum (SR) of skeletal muscle fibres through modification of the ryanodine receptor (RyR) and the sarco/endoplasmic reticulum Ca^{2+}-ATPase (SERCA), respectively. Acute pharmacological inhibition of CaMKII has an inhibitory effect on calcium release during tetanic contractions of single fast-twitch mouse fibres (Tavi et al., 2003), suggesting that CaMKII stimulates opening of the RyR. Furthermore, SERCA phosphorylation by CaMKII increases maximal activity of the slow-twitch SERCA isoform in isolated SR membranes (Hawkins et al., 1994, Xu and Narayanan, 1999). In addition, CaMKII increases SERCA activity by phosphorylating regulatory proteins sarcolipin (Bhupathy et al., 2009, Tupling et al., 2011) and phospholamban (MacLennan and Kranias, 2003). Finally, CaMKII overexpression in rat skeletal muscle *in vivo* decreased twitch contraction and relaxation times (chapter 3). These findings support the idea that the speed of calcium release and re-uptake in muscle fibres can be altered via modification of RyR and SERCA by CaMKII.

These targets, however, have a specific spatial distribution within a sarcomere. RyR is located at the terminal cisternae of the SR (Inui et al., 1987), whereas SERCA is located on the longitudinal SR (Jorgensen et al., 1982). It has been demonstrated in mouse *m. flexor digitorum brevis* fibres that the increase in cytoplasmic $[Ca^{2+}]$ after a single depolarisation depends on the location within a sarcomere, with the largest change occurring near the calcium release site, and the smallest changes near the m-line (Gomez et al., 2006). As the increase in cytoplasmic $[Ca^{2+}]$ is probably essential for contraction-induced CaMKII activation, there may also be a substantial gradient in CaMKII activity in sarcomeres. This raises the question whether CaMKII can affect SERCA, a target which is not in the immediate vicinity of the calcium release site, in skeletal muscle fibres.

We investigated whether, upon calcium release from the SR, CaMKII is activated to a greater extend when it's located in the vicinity of the RyR and whether increasing sarcomeric CaMKII concentration decreases the speed of calcium release from and re-uptake into the SR. The complexity of the required measures means that an

in vivo approach is unfeasible. We therefore coupled computational models of spatiotemporal sarcomeric [Ca^{2+}] dynamics in slow-twitch and fast-twitch fibres to models of CaMKII activation and RyR/SERCA modulation.

Methods

Description of spatiotemporal calcium dynamics model

A computational model describing spatiotemporal [Ca^{2+}] dynamics in a half sarcomere of a fast-twitch mouse muscle (Groenendaal et al., 2008) was extended with a detailed biochemical model describing CaMKII activation (Saucerman 2008). Both models consist of coupled differential equations and contain no stochastic elements. The code for the sarcomeric model was kindly provided by Dr. Willemijn Groenendaal (Eindhoven University of Technology, The Netherlands). The sarcomeric model describes a cylinder consisting of four radial layers, of which the inner three form the myoplasm and the outer layer forms the sarcoplasmic reticulum (SR). Longitudinally, the layers are divided into six parts of equal volume, to form 18 myoplasmic elements and six SR elements (Fig. 1A). The number of elements in the model was limited to 24 to prevent excessive computational times and remain within computer memory limits. The elements include buffering of calcium by troponin-C, parvalbumin (in fast-twitch muscle) and ATP in the myoplasm and calsequestrin in the SR. In the model, calcium is able to diffuse within the myoplasm and the SR, and is transported between these two compartments through the RyR and SERCA, which have distinct locations on the modelled SR (Fig. 1A).

Sarcomeres of both fast-twitch (FT) and slow twitch (ST) muscle fibres were modelled. Clear structural and biochemical differences exist between these fibre types and these were implemented as previously described (Groenendaal, 2011). In comparison with the FT model, the ST model has:

- no parvalbumin
- a 50% lower SR volume, relative to the volume of the myoplasm.
- 2.4 fold lower maximal RyR activity

- 3 fold lower maximal SERCA activity
- fewer Ca^{2+} binding sites on troponin
- 1.5 fold higher resting myoplasmic [Ca^{2+}]
- lower ATP concentration

Extension of calcium model with CaMKII reaction scheme

To each myoplasmic element in the model, we added a CaMKII reaction scheme describing Ca^{2+} binding to calmodulin (CaM) (Fig. 1B) and subsequent binding of Ca^{2+}-CaM to CaMKII (Saucerman and Bers, 2008). Six different fractions of CaMKII exist in the model (Fig. 1C): Pi (inactive), Pb2 (Ca_2CaM-bound), Pb (Ca_4CaM-bound), Pt2 (Ca_2CaM-bound and phosphorylated at Thr287), Pt (Ca_4CaM-bound and phoshorylated at Thr287) and Pa (unbound and phosphorylated at Thr287). Of these fractions, Pb, Pt2, Pt and Pa were assumed to have 100% activity. In the model, CaMKII phosphorylation is reversed by protein phosphatase 1 (PP1) (Fig. 1C).

Some modifications were made to the CaMKII reaction scheme described by Saucerman & Bers. We removed CaM-buffering from the model and modelled only free CaM. Furthermore, we used different reaction kinetic parameter values for a number of reactions, which we found to be more in agreement with available literature (Appendix). The absolute concentrations of Pi, Pb, Pb2, Pt, Pt2 and Pa, instead of concentrations normalized to total CaMKII concentration, were used to calculate reaction rates. This allowed us to investigate the effect of changes in CaMKII concentration on calcium dynamics. Isoform-specific parameters for the β-CaMKII isoform were used to describe CaM-affinity for CaMKII (Gaertner et al., 2004).

CaMKII-dependent modification of SERCA activity was implemented in the ST model as previously described for modelled cardiomyocytes (Koivumaki et al., 2009), while in the FT model regulation of SERCA activity was absent (Hawkins et al., 1994). In both the FT and the ST model, the RyR parameter 'Power1' was made dependent on the level of active CaMKII to prolong opening of the RyR in a similar way to that used for a model of cardiomyocytes (Hund and Rudy, 2004) (see Appendix). The values of KmMax and DPowermax, which describe how strongly CaMKII activity affects the activity of RyR and SERCA (Appendix), were set so that the model could reproduce the CaMKII inhibition-induced decrease in calcium release during a 70Hz

contraction, which has been previously demonstrated experimentally in single mouse fast-twitch muscle fibres (Tavi et al., 2003). The experiment by Tavi et al, which involved pharmacological inhibition of CaMKII, was modelled by removing the CaMKII-dependent modifications of RyR from our FT model. Although it was not explicitly demonstrated by Tavi et al. (2003), it was assumed that the pharmacological inhibition of CaMKII was absolute and specific. The FT values of KmMax and DPowermax were subsequently incorporated into the ST model as well, as there is no similar experimental evidence available for this muscle type.

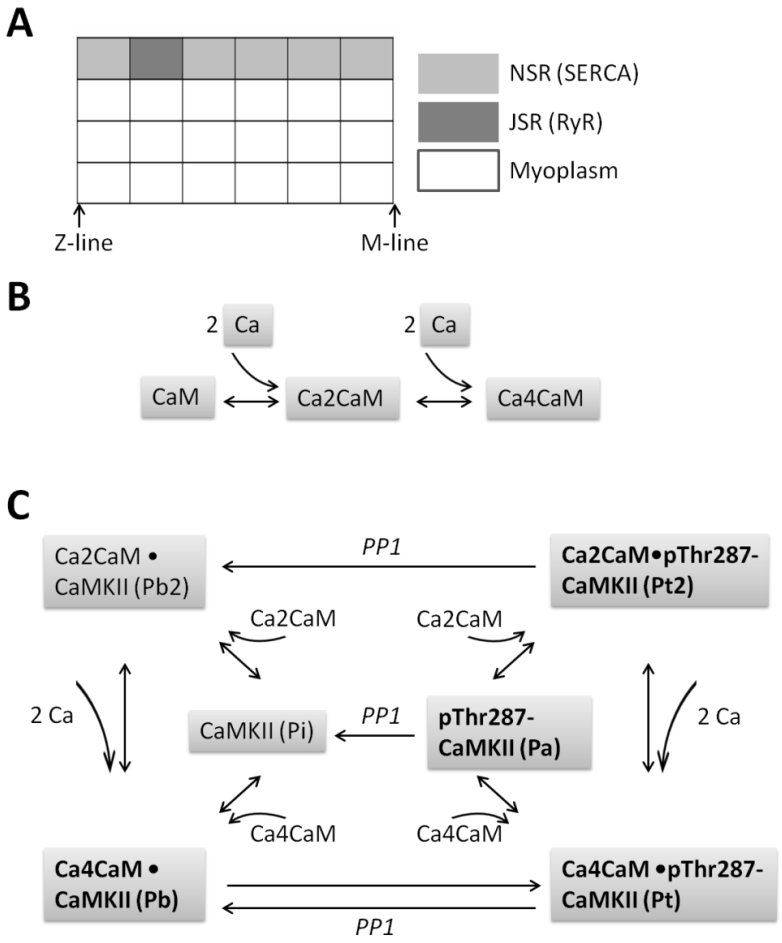

Figure 1: Schematized calcium model and CaM-CaMKII reaction schemes.

A: Simplified visualisation of the different spatial elements in the computational model of calcium dynamics in a half-sarcomere, adapted from Groenendaal et al. (2008). The model is bordered by

a z-line on one side and an m-line on the other side. The grey elements (top row) make up the SR and the white elements (bottom tree rows) make up the myoplasm. Note that the actual model is a cylinder, and the elements are actually rings, with the lower border of the bottom elements as their centre. B: Reaction scheme for sequential binding of calcium to the C-terminal and then the N-terminal EF-hand of calmodulin. C: Reaction scheme for binding of calcium and calmodulin to CaMKII, and conversion of the CaMKII fractions to a phosphorylated state. pThr287 indicates that CaMKII is phosphorylated at threonine287. Phosphorylation of CaMKII at threonine 287 in the model is reversed by the action of protein phosphatase 1 (PP1). CaMKII fractions in bold have 100% activity and the CaMKII fractions in normal font have no activity. Both CaM and CaMKII reaction schemes were adapted from Saucerman & Bers (2008). Two-way arrows indicate reversibility of the reaction. PP1: Protein phosphatase 1. Ca, CaM, Ca2CaM, Ca4CaM, Pi, Pb, Pb2, Pt, Pt2 and Pa, but not PP1, can change over time in the model. Values of reaction parameters for this reaction scheme can be found in the Appendix.

Assumptions/estimated parameter values

To the best of our knowledge, the concentration of CaMKII in skeletal muscle is unknown. We assumed a concentration of 1 µM, which has previously been used for simulations of CaMKII in skeletal muscle fibres (Tavi et al., 2003). CaMKII activity in non-stimulated muscle is 10% of maximal Ca^{2+}/CaM-stimulated activity (Rose et al., 2007a). Therefore, the initial concentration of Pa was set to 0.1 µM (see Appendix).

Total [CaM] in skeletal muscle has been estimated to be approximately 10-20 µM (Chiesi and Carafoli, 1983). However, in many cell types, CaM is presumed to be a limiting factor for calcium signalling (Persechini and Stemmer, 2002). In cardiomyocytes, most (99%) of CaM is buffered (Wu and Bers, 2007) and assumed to be unavailable for binding to CaMKII. Assuming similar CaM buffering in skeletal muscle, we set the concentration of free CaM to 0.15 µM (1% of total). [PP1] was set so CaMKII activity lasted for several tens of seconds after a simulation of 100 RyR openings, in agreement with data from chapter 2. In the model, no diffusion of any of the CaM or CaMKII fractions takes place. [CaM] and [CaMKII] were equal in all myoplasmic elements of the model, and in the FT and ST models.

Simulations were performed with Matlab (The Mathworks, v7.5.0) on an ASUS K53S laptop (2.2GHz processor, 8 GB RAM) and the ordinary differential equation (ODE) solver 15s was used. Conservation of mass during the simulations was checked.

Results

Model validation

The calcium dynamics model predicts a substantial spatial gradient in [Ca^{2+}] in sarcomeres during twitch contraction (Groenendaal et al., 2008). We compared spatially averaged [Ca^{2+}] during a simulated twitch of the FT and ST versions of the model with experimental data obtained from electrically stimulated mouse skeletal muscle fibres (Baylor and Hollingworth, 2003). The model describes rise time and peak [Ca^{2+}] amplitude of the twitch calcium peak quite well (Table 1), but the slow second half of the decrease in [Ca^{2+}] in ST fibres reported by Baylor and Hollingworth (2003) was absent in the model. Therefore, our modelled ST relaxation time was shorter than the experimentally determined relaxation time (Table 1). Adjusting the RyR opening parameters (Appendix) did not improve the modelled [Ca^{2+}] decrease time without substantial changes in the peak [Ca^{2+}]. As we judged the peak [Ca^{2+}] to be the most important parameter determining CaMKII activation, we considered the model to match the experimental data of Baylor & Hollingworth sufficiently well to model [Ca^{2+}]-dependent CaMKII activation.

	Baylor and Hollingworth (2003)		*Model*	
Parameter	**FT (EDL)**	**ST (SOL)**	**FT**	**ST**
TTP (ms)	2.0	2.5	2.0	2.1
Peak [Ca^{2+}] (µM)	21.7	8.6	20.2	8.9
HRT (ms)	2.0	4.4	1.7	1.9

Table 1: Comparison of modelled and experimental [Ca^{2+}] during one pulse stimulation

Experimental measures were carried out on single mouse muscle fibres within small bundles of fibres at 28ºC (Baylor and Hollingworth, 2003). Model results were obtained from simulations of a single RyR opening. TTP: Time-to-peak [Ca^{2+}] during a twitch. HRT: Half-relaxation time of the calcium transient during a twitch. FT: fast-twitch. ST: slow-twitch. EDL: mouse *m. extensor digitorum longus*. SOL: mouse *m. soleus*.

To validate the CaMKII reaction scheme, we first compared modelled Ca^{2+}-sensitivity of CaMKII autophosphorylation and the effect of phosphatase concentration on this relationship to that of an independent experimental dataset (Bradshaw et al., 2003). Reagent and ion concentrations, and reaction times described by Bradshaw et al. were used for these simulations. The model reproduced the concentration for half-maximal activation and steepness of the relationship between [Ca^{2+}] and CaMKII autophosphorylation quite well (Fig. 2A). Furthermore, we compared the modelled relation between [CaM] and CaMKII activity, and between [CaM] and CaMKII autophosphorylation, with another independent experimental dataset (Gaertner et al., 2004). The model properly described the experimentally determined [Ca^{2+}] concentrations for half-maximal CaMKII activity and the steepness of the curve (Fig. 2B&C).

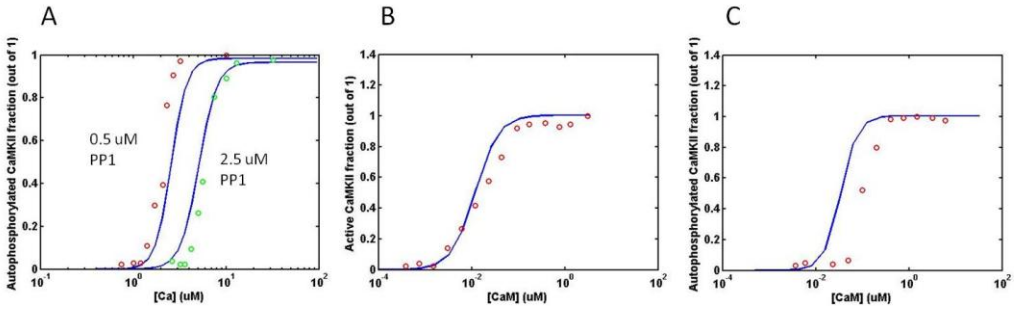

Figure 2: Validation of CaM-CaMKII reaction scheme

A: Comparison of modelled [Ca^{2+}] - phospho^{Thr287}-CaMKII relation (blue lines) with published data (red open circles: 0.5 µM PP1; green circles: 2.5 µM PP1) (Bradshaw et al., 2003). B: Comparison of modelled [CaM] - CaMKII activity relation (blue line) with independent experimental data (Gaertner et al., 2004). C: Comparison of modelled [CaM] - CaMKII autophosphorylation relation (blue lines) with independent experimental data (Gaertner et al., 2004). Experimental data points are estimated from graphs in cited papers. PP1: Protein phosphatase 1.

Simulation of prolonged repeated opening of the RyR (i.e. >100 openings) resulted in a maximum autophosphorylated (Pt, Pt2 & Pa) CaMKII fraction of 14% of total CaMKII. This is somewhat lower than the experimentally determined maximal autonomous activity of 22-23% of maximal CaMKII activity in *in situ* stimulated rat *m.*

gatrocnemius muscle (Rose et al., 2007a). However, it is in accordance with the experimentally supported idea that autonomous CaMKII activity does not exceed a ceiling of approximately 20% of maximal activity.

Effect of [Ca^{2+}] distribution on CaMKII activation

We determined maximal total CaMKII activity (defined as the sum of Pb4, Pt2, Pt4 and Pa) during simulations of single and repeated RyR openings in the FT and ST model. Furthermore, we determined whether there was an effect of RyR opening frequency on CaMKII activity, as the frequency of exposure of CaMKII to calcium/calmodulin determines the development of CaMKII activity *in vitro* (De Koninck and Schulman, 1998). CaMKII activity was determined for each myoplasmic compartment. An overview of the range of increase in CaMKII activity in the myoplasmic elements of the FT and ST models can be found in Table 2.

	FT			ST		
	Twitch	Tetanus	Train	Twitch	Tetanus	Train
10 Hz	0 - 6.5%	0.2 - 59%	3.6 - 84%	0 - 1.2%	0.2 - 29%	3.6 - 44%
100 Hz		0.5 - 95%	1.9 - 81%		0.7 - 64%	2.3 - 58%

Table 2: Increase in total CaMKII activity during single or repeated RyR openings

The range of increase in CaMKII activity in myoplasmic elements of FT and ST models from the element with the lowest increase to the element with the highest increase. Activity was determined at time points during simulations as indicated in Figures 3, 4 & 5.

As expected, the highest CaMKII activity after one simulated RyR opening occurred near the calcium release site, and no increase in activity occurred in the elements close to the m-line (Fig. 3).

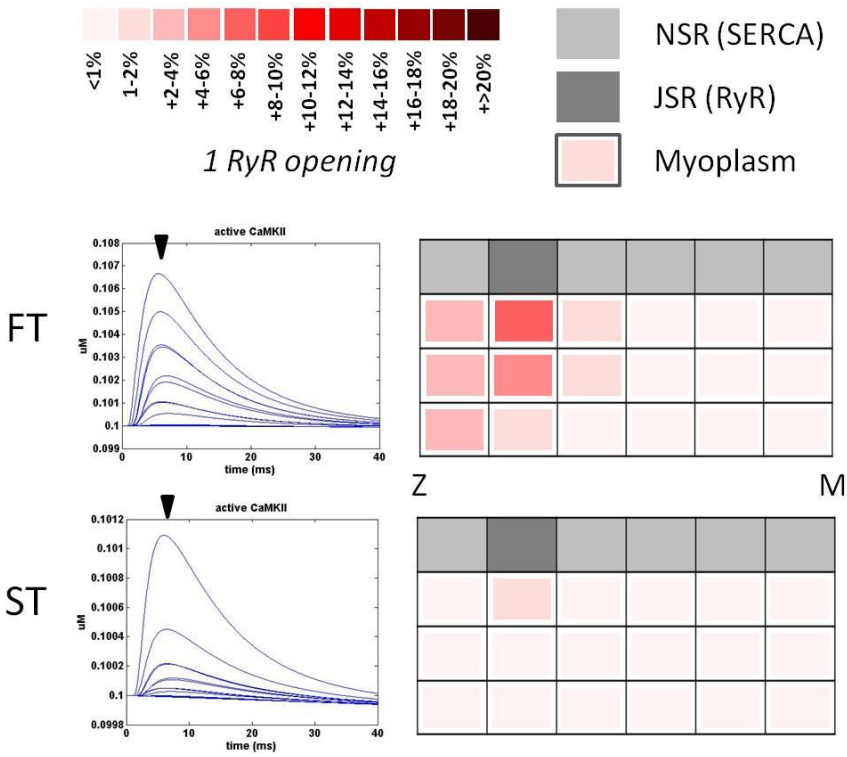

Figure 3: CaMKII activity during a single RyR opening

Total simulated CaMKII activity (the sum of Pb4, Pt2, Pt4 and Pa) during a simulated single RyR opening in the fast-twitch (FT) and slow-twitch (ST) model (see text for model details). Graphs on the left display development of total CaMKII activity over time (in milliseconds) during a single RyR opening in the FT and ST model as indicated. Blue lines represent CaMKII activity in different myoplasmic compartments. Black inverted triangles indicate the approximate time point at which the CaMKII activity gradient was analysed, and visualised in the grids on the right. Note that the scale of the y-axis differs in the FT and ST graph. Grids on the right visualise the spatial distribution of the maximal increase in total CaMKII activity during a single simulated RyR opening. Colours indicate the percentage increase compared to the initial total activity, and the scale is indicated above the figure. Grid layout is the same as in Fig. 1A. The locations of the z-line and m-line of the half-sarcomeric model are indicated by Z and M, respectively. NSR: non-junctional sarcoplasmic reticulum. JSR: junctional sarcoplasmic reticulum. SERCA: sarco/endoplasmic reticulum Ca^{2+}-ATPase. RyR: Ryanodine receptor.

We investigated whether the CaMKII activity gradient persisted when repeated RyR openings were simulated. After ten RyR openings, the spatial gradient in activity increase was stronger than after one RyR opening (Table 2, Fig. 4). However, when simulating ten repeated trains of ten RyR openings with one-second intervals between

the trains, the spatial distribution of CaMKII activity during the final ten RyR openings of the protocol is remarkably similar to that during the first ten openings. The main difference between the first and last train is an increase in baseline CaMKII activity of the most activated elements after the tenth train (Fig. 5), which is mainly due to the increase in fraction Pa, the autonomous CaMKII activity. Nevertheless, in all cases CaMKII activation was highest near the calcium release site and higher in the elements closest to the z-line than in the elements closest to the m-line (Fig. 3). These data suggest that CaMKII activity is highest in the vicinity of the calcium release site during muscle contractions.

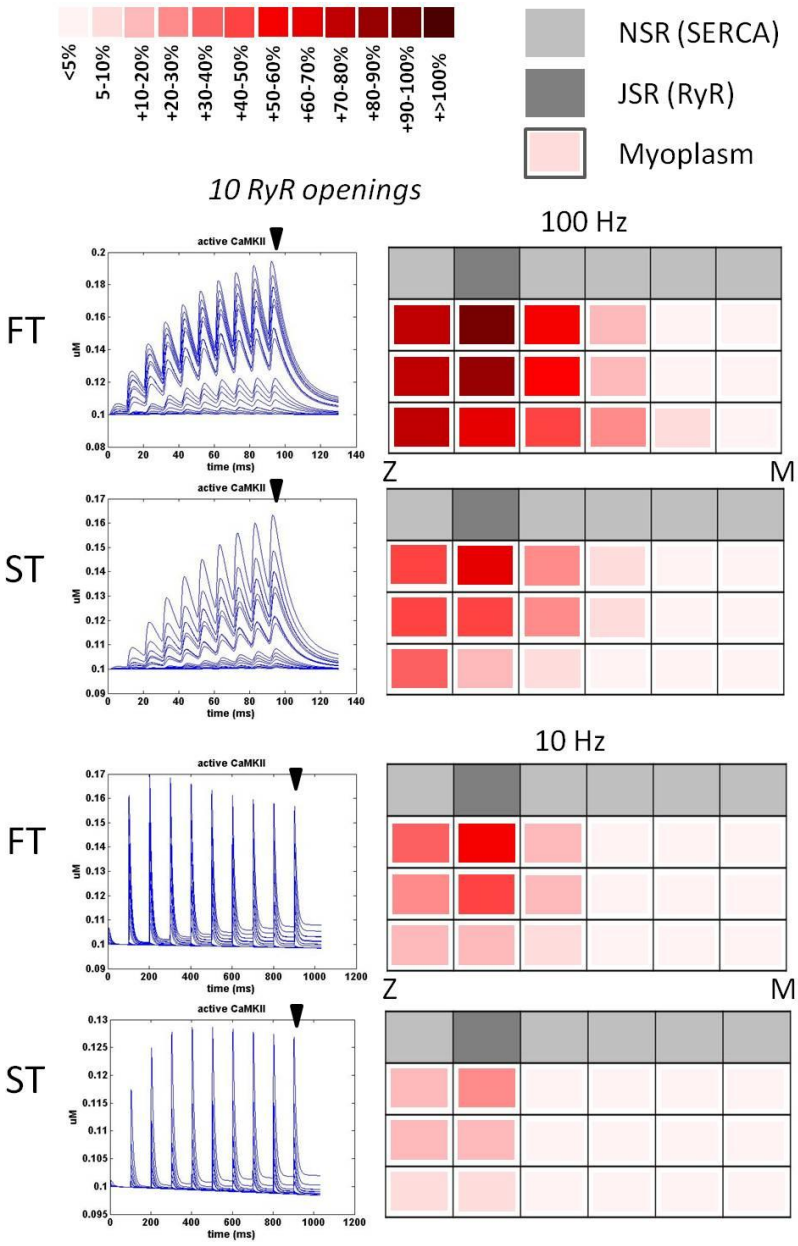

Figure 4: CaMKII activity during repeated RyR openings

Total simulated CaMKII activity (the sum of Pb4, Pt2, Pt4 and Pa) during a simulation of ten RyR openings in the fast-twitch (FT) and slow-twitch (ST) model (see text for model details). Graphs on the left display development of total CaMKII activity over time (in milliseconds) during ten simulated RyR openings in FT and ST model as indicated, and at a RyR opening frequency of 100Hz (upper two graphs) or 10Hz (lower two graphs). Blue lines represent CaMKII activity in different myoplasmic compartments. In order to optimise visualisation of the graphs, the scale of

the y-axis differs in each graph. Black inverted triangles indicate the approximate time point at which the CaMKII activity gradient was analysed, and visualised in the grids on the right. Grids on the right visualise the spatial distribution of maximal total CaMKII activation during the simulation of ten RyR openings. Colours indicate the percentage increase compared to the initial total activity, and the scale is indicated above the figure. Note that colour scale in this figure is of larger magnitude compared to Fig. 3. Grid layout is the same as in Fig. 1A. The locations of the z-line and m-line of the half-sarcomeric model are indicated by Z and M, respectively. NSR: non-junctional sarcoplasmic reticulum. JSR: junctional sarcoplasmic reticulum. SERCA: sarco/endoplasmic reticulum Ca2+-ATPase. RyR: Ryanodine receptor.

Models of FT and ST sarcomeres were used to investigate whether CaMKII activation differs between these muscle types. CaMKII activation was higher in the FT model compared to the ST model after single and repeated RyR openings (Table 2, Fig. 3, 4 & 5). This is associated with a higher peak [Ca^{2+}] amplitude in the FT model (Table 1), and in partial agreement with experimental data demonstrating that phospho^{Thr287}-CaMKII levels increase in fast-twitch, but not slow-twitch rat muscle after electrical stimulation with 100 electrical pulses *in situ* (chapter 2).

To investigate whether RyR opening frequency affects CaMKII activation, we simulated repeated RyR openings at both 10 Hz and 100 Hz. After ten RyR openings, CaMKII activation was substantially higher when RyR opening occurred at 100 Hz compared to 10 Hz (Table 2, Fig. 4). However, after ten trains of RyR openings, this difference between the frequencies had disappeared in the FT model and was reduced in the ST model (Table 2, Fig. 5). This was in agreement with experimental data demonstrating no effect of frequency on phospho^{Thr287}-CaMKII levels after *in situ* stimulation of rat skeletal muscle with 100 electrical pulses at 10 or 150 Hz (Chapter 2). These data suggest that a low frequency of RyR opening results in lower CaMKII activation during the initial openings, but that as RyR opening continues, the CaMKII activation during low frequency RyR opening eventually matches that during high-frequency RyR opening, and is not likely to be a factor during repeated muscle contractions.

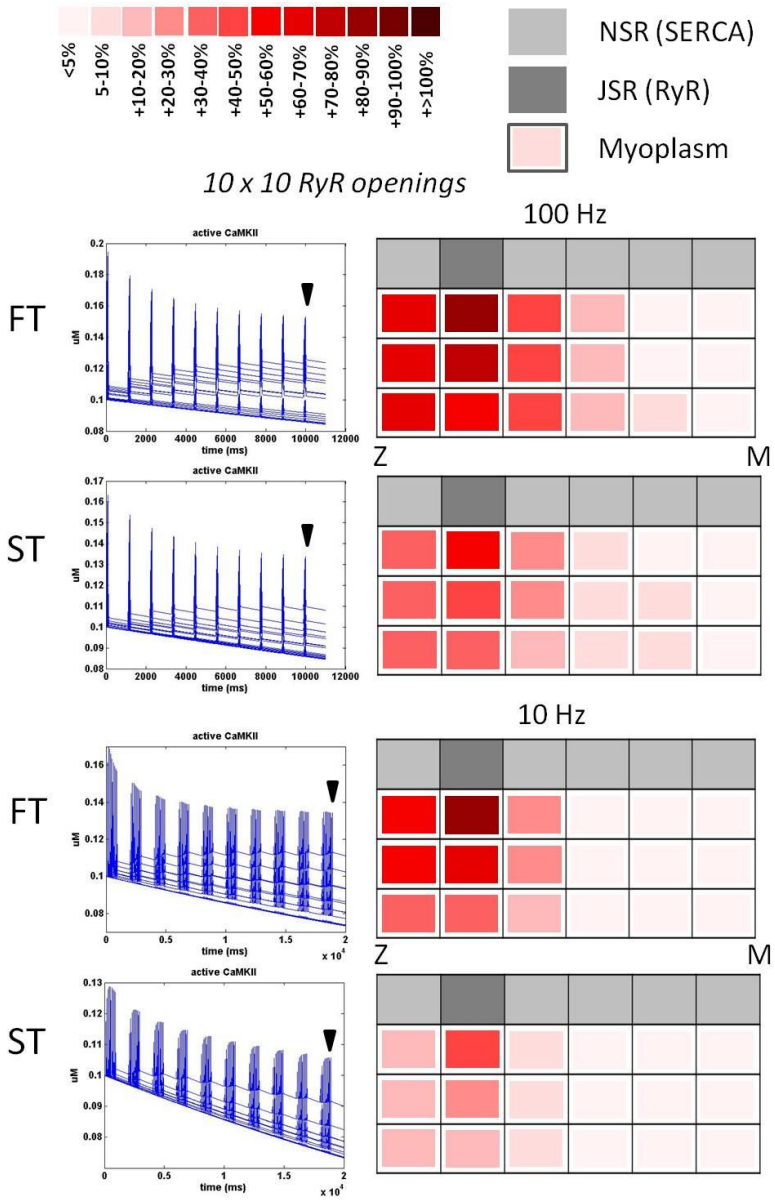

Figure 5: CaMKII activity during repeated trains of RyR openings

Total CaMKII activity (the sum of Pb4, Pt2, Pt4 and Pa) during a simulation of 10 x 10 RyR openings in the fast-twitch (FT) and slow-twitch (ST) model (see text for model details). Graphs on the left display development of total CaMKII activity over time (in milliseconds) during the 10 x 10 RyR openings protocol in FT and ST model as indicated, and at a RyR opening frequency of 100Hz (upper two graphs) or 10Hz (lower two graphs). The interval between each train of ten RyR openings was one second. Blue lines represent CaMKII activity in different myoplasmic compartments. In order to optimise visualisation of the graphs, the scale of the y-axis differs in

each graph. Black inverted triangles indicate the approximate time point at which the CaMKII activity gradient was analysed, and visualised in the grids on the right. The decreasing baseline CaMKII activity can be attributed to PP1 activity, but is adjusted for when calculating the increase in activity in each myoplasmic element. Grids on the right visualise the spatial distribution of maximal total CaMKII activation during the final 10 pulses of the simulation protocol. Colours indicate the percentage increase compared to the initial total activity, and the scale is indicated above the figure. Note that the colour scale in this figure is the same as that in Fig. 4, but of a larger magnitude compared to Fig. 3. Grid layout is the same as in Fig. 1A. The locations of the z-line and m-line of the half-sarcomeric model are indicated by Z and M, respectively. NSR: non-junctional sarcoplasmic reticulum. JSR: junctional sarcoplasmic reticulum. SERCA: sarco/endoplasmic reticulum Ca^{2+}-ATPase. RyR: Ryanodine receptor.

Effect of CaMKII concentration on calcium dynamics in FT and ST fibres

We used the model to investigate the effect of increased CaMKII concentration, which has been shown to increase relaxation speed in rat skeletal muscle (chapter 3), on calcium dynamics. CaMKII concentration was increased 50-fold in each myoplasmic element. This increased the local concentrations of total active CaMKII during a simulation of a single RyR opening compared to the same simulation with 'normal' CaMKII concentration (Fig. 6A/C). This increase occurred mainly in the elements closest to the RyR. However, it had no effect on the development of the [Ca^{2+}] or calcium-bound troponin-C concentration ([Ca^{2+}-TropC]) over time in the FT and ST model (Fig. 6B/D).

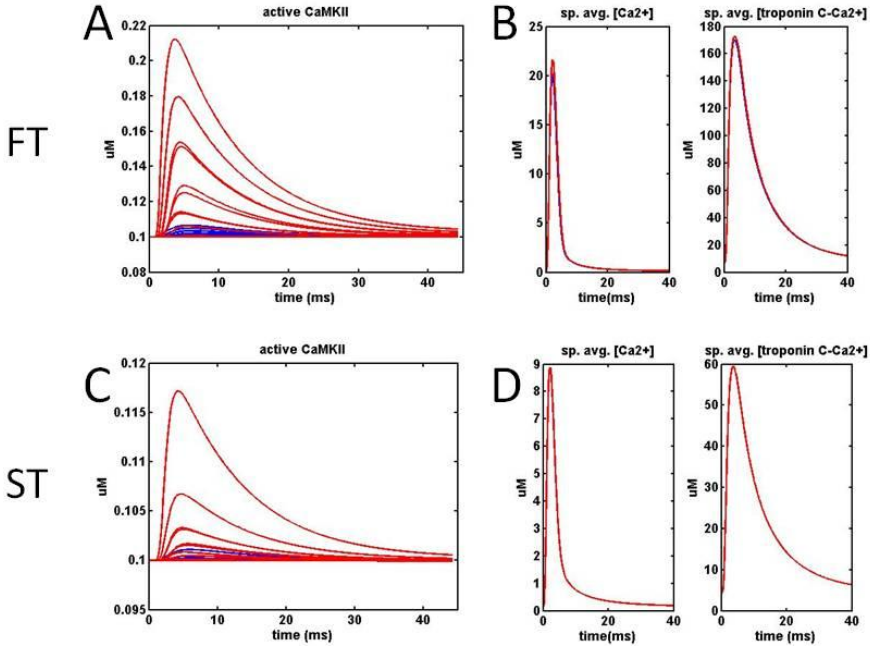

Figure 6: The effect of increased CaMKII levels on twitch characteristics

A/C: Total CaMKII activity (the sum of Pb, Pt, Pt2 and Pa) during a simulation of a single RyR opening in the fast-twitch (FT; A) and slow-twitch (ST; C) model in which CaMKII concentration is increased. Lines indicate CaMKII activity in different myoplasmic compartments. Blue lines: [CaMKII] = 1 µM; Red lines: [CaMKII] = 50 µM. Note that the scales on the y-axes are different. B/D: Spatially averaged [Ca^{2+}] (left graphs) and [Ca^{2+}-TropC] (right graphs) during a simulation of one RyR opening in the FT (B) and ST (D) model. Blue lines: [CaMKII] = 1 µM; Red lines: [CaMKII] = 50 µM. Note that scales on the y-axes are different.

An alternative explanation for the experimentally observed increase in relaxation speed is an increase in SERCA expression (chapter 3). When increasing maximal SERCA activity in the model by two-fold to reflect increased SERCA protein level, [Ca^{2+}] and [Ca^{2+}-TropC] were reduced during the relaxation phase of the twitch (Fig. 7 B/D). These data suggest that the decrease in relaxation time when CaMKII is overexpressed in rat skeletal muscle cannot be explained by CaMKII-induced increases in SERCA activity, but can be at least partially explained by increased SERCA expression levels.

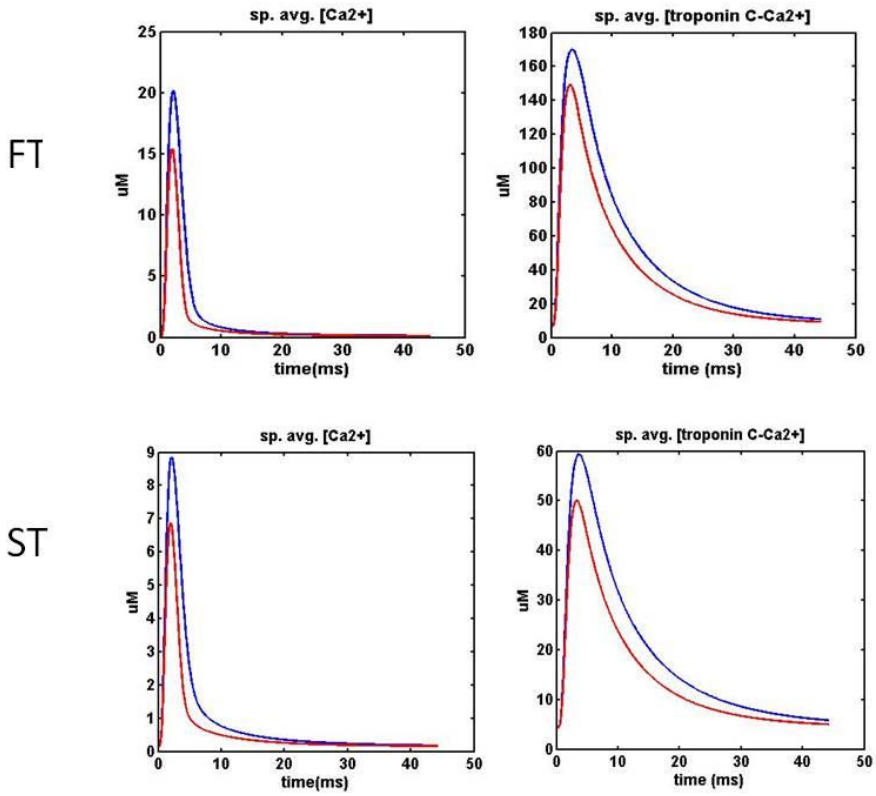

Figure 7: The effect of increasing SERCA levels on twitch characteristics

Spatially averaged [Ca^{2+}] (left graphs) and [Ca^{2+}-TropC] (right graphs) during a simulation of a single RyR opening in the fast-twich (FT) and slow-twitch (ST) model. Blue lines: SERCA activity = normal; Red lines: SERCA activity = 2 x normal. Note that scales on the y-axes are different.

Discussion

Main findings

We aimed to investigate whether CaMKII might be differentially activated within a sarcomere depending on its subsarcolemmal location and whether decreases in twitch contraction and relaxation times after CaMKII overexpression can be explained by CaMKII-dependent modification of RyR and SERCA. We found that the modelled spatial gradient in cytoplasmic [Ca^{2+}] results in a two-fold decrease in CaMKII activity

between the Ca^{2+} release site (i.e. near the z-line) and the part of the sarcomere close to the m-line. This gradient existed during simulations of a single RyR opening and simulations of repeated trains of RyR opening (Fig. 3, 4 & 5). Furthermore, simulated CaMKII activity increased more in the FT model than in the ST model (Fig. 3, 4 & 5). Finally, we found that CaMKII-dependent modulation of RyR and SERCA cannot explain CaMKII overexpression-induced decreases in twitch contraction and relaxation times (Fig. 6).

Model limitations

RyR and SERCA are both influenced by a plethora of interacting factors (Zalk et al., 2007, Vangheluwe et al., 2005), which were not modelled because of the lack of quantitative descriptions of their effects. It is unknown whether these factors might mediate or influence CaMKII-dependent effects on RyR or SERCA.

Direct modification of RyR by a calcium/calmodulin-dependent protein kinase-dependent phosphorylation has been shown to inhibit RyR opening in isolated SR membrane patches of frog skeletal muscle (Wang and Best, 1992). In contrast, pharmacological inhibition of CaMKII in single mouse skeletal muscle fibres resulted in decreased calcium release during tetanic stimulation (Tavi et al., 2003), which suggests the effect of CaMKII on calcium release is stimulatory. We valued the latter study more, as the data were obtained from intact fibres with intact SR which may include CaMKII-RyR interactions which are no longer present in isolated membrane patches. Therefore, we modelled a stimulatory effect of CaMKII on RyR.

To the best of our knowledge, the exact concentrations of CaM, CaMKII and PP1 in skeletal muscle fibres are unknown. PP1 concentration was set based on experimental results demonstrating that CaMKII phosphorylation can persist for up to two minutes after stimulation of rat skeletal muscle with 100 pulses (chapter 2). The effects of CaM concentration on global CaMKII activity in the model indicated that this is an important determinant of CaMKII activity (Fig. 8). Although increasing the concentration of CaMKII and CaM in the model increased the absolute levels of active CaMKII, a spatial gradient in CaMKII activity still existed (see Fig. 6A/C for the effect of increased CaMKII concentration). In addition, increasing the CaM concentration two-fold in the model did not affect the conclusion that CaMKII-dependent

modification of RyR and SERCA was not sufficient to affect the speed of calcium release and re-uptake (Fig. 8).

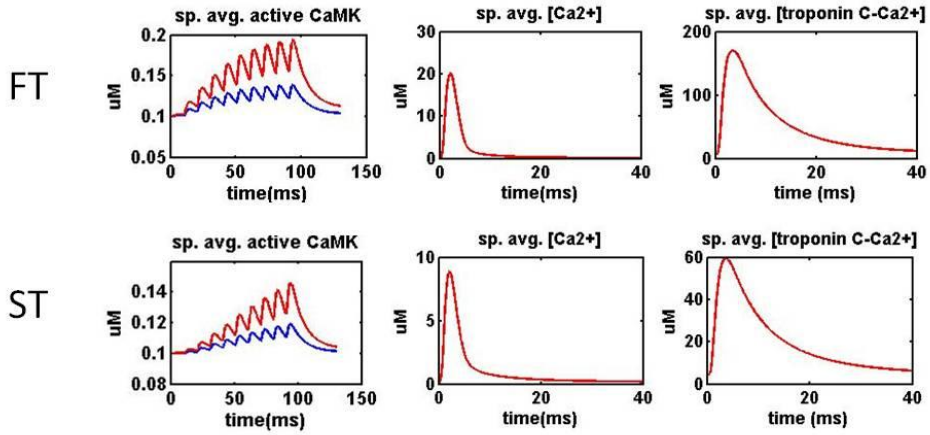

Figure 8: Effect of increased calmodulin concentration on CaMKII activity and calcium release
Spatially averaged [active CaMKII] during a simulation of 10 repeated pulses at 100 Hz, and spatially averaged [Ca^{2+}] and [Ca^{2+}-TropC] during a simulation of a single RyR opening in the fast-twich (FT) and slow-twitch (ST) models. Blue lines: [CaM] = 0.15µM. Red lines: [CaM] = 0.30 µM. Note that scales on the y-axes are different between graphs for FT and ST models.

The experimentally determined effect of CaMKII overexpression on muscle twitch relaxation was derived from muscle force traces (chapter 3). Although our model predicted that a CaMKII-dependent increase in SERCA expression (chapter 3) leads to a decrease in calcium twitch time, the development of force by cross-bridges was not modelled. Therefore, it is unclear to what extend the modelled change in calcium dynamics in the model translate into a change in force dynamics. However, as differences in calcium dynamics are presumed to underlie the difference in twitch time between FT and ST muscle (Schiaffino, 2010), the modelled decrease in calcium twitch time is likely to have an effect on muscle force dynamics.

Implications of modelling results for the function of CaMKII in skeletal muscle
CaMKII has many substrates and one mechanism to achieve signalling specificity is physical targeting of the kinase to its substrates (Bayer and Schulman, 2001). As our

model predicted that the spatial gradients in CaMKII activity persist during repeated RyR openings, CaMKII substrates in skeletal muscle fibres will be differentially regulated by CaMKII, dependent on their subsarcolemmal location (Table 2; Fig. 3, 4, & 5).

RyR is located at the terminal cisternae of the SR (Inui et al., 1987), whereas SERCA is located on the longitudinal SR (Jorgensen et al., 1982). CaMKII is targeted to the SR by a non-kinase splice variant of the α-CaMKII isoform, αKAP (Bayer et al., 1998). αKAP co-localises with SERCA2 to the longitudinal SR in mouse *m. soleus* fibres (Nori et al., 2003), suggesting that CaMKII may be physically targeted to SERCA. Furthermore, CaMKII is located at the terminal SR in the vicinity of the RyR (Chu et al., 1990). Thus, CaMKII appears to be spatially targeted to these targets. As CaMKII activity is highest at the site of RyR, and barely activated at a fraction of the elements that contain SERCA, CaMKII-dependent regulation of RyR in muscle fibres may be stronger compared to that of SERCA, or the SERCA-associated regulatory proteins phospholamban and sarcolipin.

Similarly, local CaMKII activation could have implications for CaMKII-dependent regulation of other substrates. CaMKII was found to both complex with, and phosphorylate, glyceraldehyde 3-phosphate dehydrogenase, glycogen phosphorylase, glycogen debranching enzyme and creatine kinase in SR-membranes, (Singh et al., 2004). It is unclear whether this complex is located in the immediate vicinity of RyR, where it would be most strongly activated.

Interestingly, β-CaMKII, including the muscle specific β_m isoform, binds to f-actin in biochemical essays as well as in cultured neuronal cells, an interaction which has been shown to be inhibited by Ca^{2+}/CaM-binding (Shen et al., 1998, O'Leary et al., 2006, Sanabria et al., 2009). As our simulations suggest that the actin filaments of sarcomeres are located in the region where Ca^{2+}/CaM-binding to CaMKII takes place (Fig.s 3, 4 & 5), this raises the question whether CaMKII might regulate actin assembly or bundling in skeletal muscle. However, CaMKII binding to actin in skeletal muscle has not yet been demonstrated, and this could be an interesting area for future research.

Overexpression of CaMKII in rat skeletal muscle increases the speed of twitch contraction and relaxation (chapter 3). When we increased the CaMKII concentration in the model, the calcium and calcium-bound troponin-C concentration dynamics during a

single RyR opening did not differ from that predicted by the simulation with 'normal' CaMKII concentration (Fig. 6). The results of our simulation suggest that CaMKII is barely activated during one pulse (Fig. 3), which explains the absence of differences between the simulations with different CaMKII concentrations. CaMKII overexpression increased SERCA2 expression in rat skeletal muscle (chapter 3). In contrast to only increasing [CaMKII], additionally increasing maximal SERCA activity in the model caused an earlier decrease in [Ca^{2+}] and [Ca^{2+}-TropC] (Fig. 7B/D). Therefore, increased SERCA expression may partially explain the increased relaxation speed observed in CaMKII-overexpressing rat muscles (chapter 3).

Although CaMKII activation was highest near the RyR, increasing [CaMKII] in the model did not result in a faster rise in [Ca^{2+}] in the model (Fig. 6B/D). This is unlikely to be related to insufficient CaMKII activity, as increasing baseline CaMKII activity by 50-fold in the model only resulted in an approximate doubling of the peak [Ca^{2+}] amplitude, but not a decrease in time to peak [Ca^{2+}] or [Ca^{2+}-TropC] (Fig. 9). More likely, the absence of an effect of increased [CaMKII] on [Ca^{2+}] rise time is related to the fact that the description of RyR in the model and its modification by CaMKII (Appendix) lacks the relevant components required to model the physiological effect of CaMKII on the RyR.

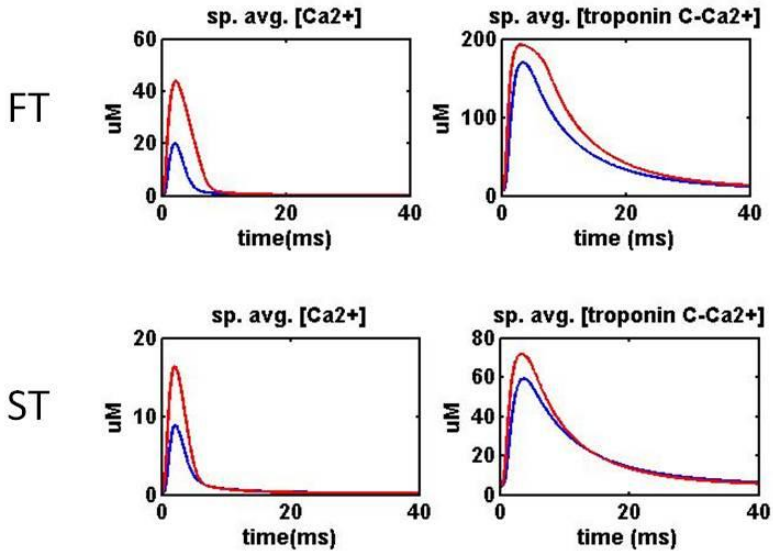

Figure 9: Effect of increased basal CaMKII activity on sarcomeric calcium release
Spatially averaged [Ca^{2+}] (left graphs) and [Ca^{2+}-TropC] (right graphs) during a simulation of a single RyR opening in the fast-twich (FT) and slow-twitch (ST) model. Blue lines: basal [active CaMKII] = 0.1µM. Red lines: basal [active CaMKII] = 5.0µM. Note that scales on the y-axes are different.

Finally, we argue that the existence of a spatial gradient in CaMKII activity also has implications for the use of constitutively active mutants when using transgenic/overexpression approaches to investigate the function of CaMKII, as these introduce CaMKII activity distributed throughout the entire cell, and may therefore also introduce phosphotransfer activity to substrates that would normally not receive this.

Conclusion

The model is a useful tool to investigate CaMKII signalling towards its targets in skeletal muscle sarcomeres when reaction kinetic information regarding their activation becomes available. Our modelling of CaMKII activity in skeletal muscle sarcomeres and its effects show CaMKII is locally activated, and its spatial activity gradient is maintained during repeated stimulation. Therefore, the location of CaMKII in a

sarcomere is likely to be of importance for its function and should be considered when evaluating potential CaMKII targets for physiological relevance.

Appendix: Reaction parameter values

Reaction rate calculations

Reaction rates for the CaM and CaMKII reaction schemes were calculated as in Saucerman &Bers (2008), with the modification of using absolute concentrations of Pi, Pb, Pb2, Pt, Pt2 and Pa. Some reactions were excluded as described in the methods section. Values of the reaction parameters can be found in the tables below.

Calcium-calmodulin binding

Parameter	Description	Value	Reference
CaMFreeR	Free CaM concentration	0.15 µM	(Chiesi and Carafoli, 1983)
Mg	Myoplasmic Mg2+ concentration	1 µM	(Jones et al., 2004)
K	Myoplasmic K+ concentration	160 µM	(Sejersted and Sjogaard, 2000)
Kd02	-	14.546	(Saucerman and Bers, 2008)
Kd24	-	836.69	(Saucerman and Bers, 2008)
k20	2 Ca dissociation from CaM (C-terminal)	10 s^{-1}	(Saucerman and Bers, 2008)
k02	2 Ca binding to CaM (C-terminal)	k20/Kd02 μM^{-2} s^{-1}	(Saucerman and Bers, 2008)
k42	2 Ca dissociation from CaM (N-terminal)	500 s^{-1}	(Saucerman and Bers, 2008)
k24	2 Ca binding to CaM (N-terminal)	k42/Kd24 μM^{-2} s^{-1}	(Saucerman and Bers, 2008)

Table 2: Reaction parameters for calcium-calmodulin binding

CaMKII reactions

Parameter	Description	Value (units)	Reference
CaMKIItot	Total CaMKII concentration	1 µM or 50 µM	-
PiR	Initial inactive CaMKII fraction	0.9	-
PbR	Initial Ca4CaM-bound CaMKII fraction	0	-
Pb2R	Initial Ca2CaM-bound CaMKII fraction	0	-
PtR	Initial Ca4CaM-bound pThr287-CaMKII fraction	0	-
Pt2R	Initial Ca2CaM-bound pThr287-CaMKII fraction	0	-
PaR	Initial unbound pThr287-CaMKII fraction	0.1	(Rose et al., 2007a)
PP1tot	Total PP1 concentration	0.1 µM	-
Kbi	Ca4CaM dissociation from Pb	0.54 s^{-1}	(Gaertner et al., 2004)
Kib	Ca4CaM binding to Pb	kbi/25.7e-3 $\mu M^{-1}s^{-1}$	(Gaertner et al., 2004)
kb2i	Ca2CaM dissociation from Pb2	14*kbi s^{-1}	(Shifman et al., 2006)
kib2	Ca2CaM binding to Pb2	Kbi $\mu M^{-1}s^{-1}$	-
kb42	2 Ca dissociation from Pb	k42/5 s^{-1}	(Shifman et al., 2006)
kb24	2 Ca binding to Pb2	k24 $\mu M^{-2}s^{-1}$	-
Kta	Ca4CaM dissociation from Pt	kbi/1000 s^{-1}	(Meyer et al., 1992)
Kat	Ca4CaM binding to Pt	kib $\mu M^{-1}s^{-1}$	(Meyer et al., 1992)
kt2a	Ca2CaM dissociation from Pt	14*kta s^{-1}	(Shifman et al., 2006)
kat2	Ca2CaM binding to Pt	kib $\mu M^{-1}s^{-1}$	-
kt42	2 Ca dissociation from Pt	k42/5 s^{-1}	-
kt24	2 Ca binding to Pt2	k24 $\mu M^{-2}s^{-1}$	-
kPP1	Thr287 dephosphorylation	1.72 s^{-1}	(Saucerman and Bers, 2008)
KmPP1	Km for Thr287 dephosphorylation	11 µM	(Bradshaw et al., 2003)

Table 3: Reaction parameters for the CaMKII reaction scheme

CaMKII-dependent modification of RyR and SERCA

FT model

$RyR = ([Ca]_{JSR} - [Ca]_{MYO}) * CaMax * (1-e^{(-t/tau1)})^{(Power1-DPowermax)} * (e^{(-t/tau2)})^{Power2}$

$SERCA = CaPump * [Ca]^2 / ([Ca]^2 / KdPump^2)$

ST model

RyR: as in FT model

$CaMKIIreg = CaMKactive^3 / (KmCaMK^3 + CaMKactive^3)$

$SERCA = (Jmax\_up * CaMKIIreg + 1) * CaPump * [Ca]^2 / ([Ca]^2 / KdPump^2)$

Parameter	Description	Value (units)	Reference
CaMax	Maximum RyR activity	FT: $6.981*10^5$ ST: $2.9088* 10^5$	- -
Tau1	RyR opening parameter	FT: 1.11 ST:1.1	(Groenendaal et al., 2008) -
Tau2	RyR opening parameter	FT: 1.4074 ST:1.5	(Groenendaal et al., 2008) -
Power1	RyR opening parameter	FT: 5 ST:5.2	(Groenendaal et al., 2008) -
Power2	RyR opening parameter	FT: 3 ST:3	(Groenendaal et al., 2008) -
CaPump	Maximum SERCA activity	FT: 170.2749 ST: 56.7583	(Groenendaal et al., 2008) (Groenendaal et al., 2008)
KdPump	$[Ca^{2+}]$ at which SERCA activity is half-maximal	FT: 1 µM ST: 1 µM	(Groenendaal et al., 2008) (Groenendaal et al., 2008)
CaMKactive	Total concentration of active CaMKII	Pb+Pt2+Pt+Pa µM	
KmCaMK	Concentration of active CaMKII at which effect on substrates is 50% of maximum effect	0.2 µM	-

Jmax_up	Maximal % increase in KdPump	70%	(Hund and Rudy, 2004)
DPower1max	Maximal % increase in Power 1	30%	-

Table 4: Parameters related to RyR and SERCA activity and their CaMKII-dependent modification